Structural and mechanistic insights into the activation of Stromal interaction molecule 1 (STIM1)

Xue Yang[a,b,1], Hao Jin[a,b,1], Xiangyu Cai[c,1], Siwei Li[a,b], and Yuequan Shen[a,b,2]

[a]State Key Laboratory of Medicinal Chemical Biology, [b]College of Life Sciences, and [c]School of Medicine, Nankai University, Tianjin 300071, China

Edited by Richard W. Aldrich, University of Texas at Austin, Austin, TX, and approved February 7, 2012 (received for review November 17, 2011)

Calcium influx through the Ca^{2+} release-activated Ca^{2+} (CRAC) channel is an essential process in many types of cells. Upon store depletion, the calcium sensor in the endoplasmic reticulum, STIM1, activates Orai1, a CRAC channel in the plasma membrane. We have determined the structures of SOAR from *Homo sapiens* (hSOAR), which is part of STIM1 and is capable of constitutively activating Orai1, and the entire coiled coil region of STIM1 from *Caenorhabditis elegans* (ceSTIM1-CCR) in an inactive state. Our studies reveal that the formation of a SOAR dimer is necessary to activate the Orai1 channel. Mutations that disrupt SOAR dimerization or remove the cluster of positive residues abolish STIM1 activation of Orai1. We identified a possible inhibitory helix within the structure of ceSTIM1-CCR that tightly interacts with SOAR. Functional studies suggest that the inhibitory helix may keep the C-terminus of STIM1 in an inactive state. Our data allowed us to propose a model for STIM1 activation.

crystal structure | SOAR | store-operated calcium entry | Stromal interaction molecule

Calcium signaling plays an essential role in many biological processes (1). Store-operated Ca^{2+} entry (SOCE) is a critical cellular signaling pathway in immune cells (2, 3). The molecular mechanism underlying SOCE remained elusive for more than two decades until the recent discovery of two key components, the Stromal interaction molecule (STIM) (4, 5) and Orai, a Ca^{2+}-release-activated Ca^{2+} (CRAC) channel (6–8). The binding of extracellular ligands to receptors on the plasma membrane (PM) initiates a series of signaling events and stimulates the production of inositol-1,4,5-triphosphate, leading to Ca^{2+} release from the endoplasmic reticulum (ER) (9–11). The depletion of Ca^{2+} from the ER causes the oligomerization of STIM1 and further triggers the opening of Orai1. Influx of Ca^{2+} through the CRAC channel regulates the biological function of numerous targets and eventually leads to various cellular responses (2, 3, 12). Consequently, mutations in STIM1 directly result in hereditary immunodeficiencies in humans (2).

Besides acting as a calcium stress sensor, STIM1 has recently been reported to be a sensor of oxidative stress (13) and temperature variation stress (14), indicating that STIM1 may act as a general stress sensor that orchestrates calcium signaling in the cell (15). Human STIM1 has 685 amino acids and consists of an approximately 22 kDa N-terminal portion (STIM1-N) located in the ER lumen, a single transmembrane segment and an approximately 51 kDa C-terminal portion (STIM1-C) in the cytoplasm (2). The STIM1-N can be further divided into tandem EF-hand and sterile alpha motif domains (16), whereas the STIM1-C encompasses two coiled-coil domains, a Pro/Ser-rich domain and a Lys-rich domain (17). Structural investigation and biochemical evidence revealed that STIM1-N alone was capable of promoting the transition of itself from a monomer to an oligomer upon release of Ca^{2+} from the first EF-hand of STIM1-N; this release is thought to be an initiation event for capacitive Ca^{2+} entry (16, 18). STIM1-C is responsible for the relocalization of STIM1 oligomers to the ER-PM junctions and directly binds to Orai1 (19–21, 23). Although the entire STIM-C poorly activates Orai1, previous studies have identified cytosolic regions within STIM1-C, defined as the STIM1 Orai1-activating region (SOAR, amino acids 344–442) or the CRAC activation domain (CAD, amino acids 342–448) or coiled-coil domain containing region b9 (CCb9, amino acids 339–444), that are essential for oligomerization (11) and capable of constitutively activating Orai1 (22–24). Therefore, STIM1-C presumably remains inactive in a resting state and adopts conformational changes to become active. Indeed, several studies have proposed that intramolecular inhibition in STIM1 prevents the expose of the SOAR (25, 26). However, the absence of structural data has hindered further understanding of this crucial process.

Here, we describe the atomic structures of both the SOAR from *Homo sapiens* (hSOAR) and the entire coiled-coil region of STIM1-C from *Caenorhabditis elegans* (ceSTIM1-CCR). Our results elucidate the molecular basis for STIM1 activation.

Results

Overall Structure of hSOAR. Wild-type hSOAR is notoriously difficult to purify. Thus, a series of hSOAR mutants were expressed, purified and subjected to crystallization trials. One hSOAR mutant (amino acids 345–444 with three mutations L374M, V419A, and C437T, designated as hSOAR-MAT) yielded good-quality crystals that diffracted to high resolution. These MAT mutations do not affect the biological function of hSOAR or full-length human STIM1 (hSTIM1) in terms of colocalization with human Orai1 (hOrai1) or $Ca_v1.2$ channels and SOCE (Fig. S1). The structure of hSOAR-MAT was determined with single wavelength anomalous dispersion (SAD). The entire structure resembles the capital letter "R" (Fig. 1 *A* and *B*). It consists of a total of four α-helices, with two long α-helices in the N-and C-terminal regions and two short α-helices in the middle. Sequence alignment of SOAR from various species shows that the amino acids are highly conserved (Fig. S2), indicating potential conservation in both the three-dimensional structure and biological function. One asymmetric unit cell consists of four molecules of hSOAR. Two of the molecules are fully defined, whereas a lack of electron density prevents modeling the last C-terminal residue in the other two molecules. Overall, the four molecules in the asymmetric unit are highly similar with a root-mean-square deviation (r.m.s.d.) of less than 0.95 Å for 99 pairwise C-alpha atoms.

Packing of the hSOAR Dimer. A previous report showed that a construct of hSTIM1 (residues 336–485), which is longer than hSOAR, exists as a dimer in solution (22). Accordingly, we also found by analytical ultracentrifugation (Fig. S3) that wild-type hSOAR exists mainly as a dimer and partially as a tetramer in

Author contributions: Y.S. designed research; X.Y., H.J., X.C., and S.L. performed research; X.Y. and Y.S. analyzed data; and X.Y. and Y.S. wrote the paper.

The authors declare no conflict of interest.

This article is a PNAS Direct Submission.

Data deposition: The atomic coordinates and structure factors for the reported crystal structures have been deposited in the Protein Data Bank, www.pdb.org [PDB ID codes 3TEQ (hSOAR) and 3TER (ceSTIM1-CCR)].

[1]X.Y., H.J., and X.C. contributed equally to this work.

[2]To whom correspondence should be addressed. E-mail: yuequan74@yahoo.com.

This article contains supporting information online at www.pnas.org/lookup/suppl/doi:10.1073/pnas.1118947109/-/DCSupplemental.

BIOCHEMISTRY

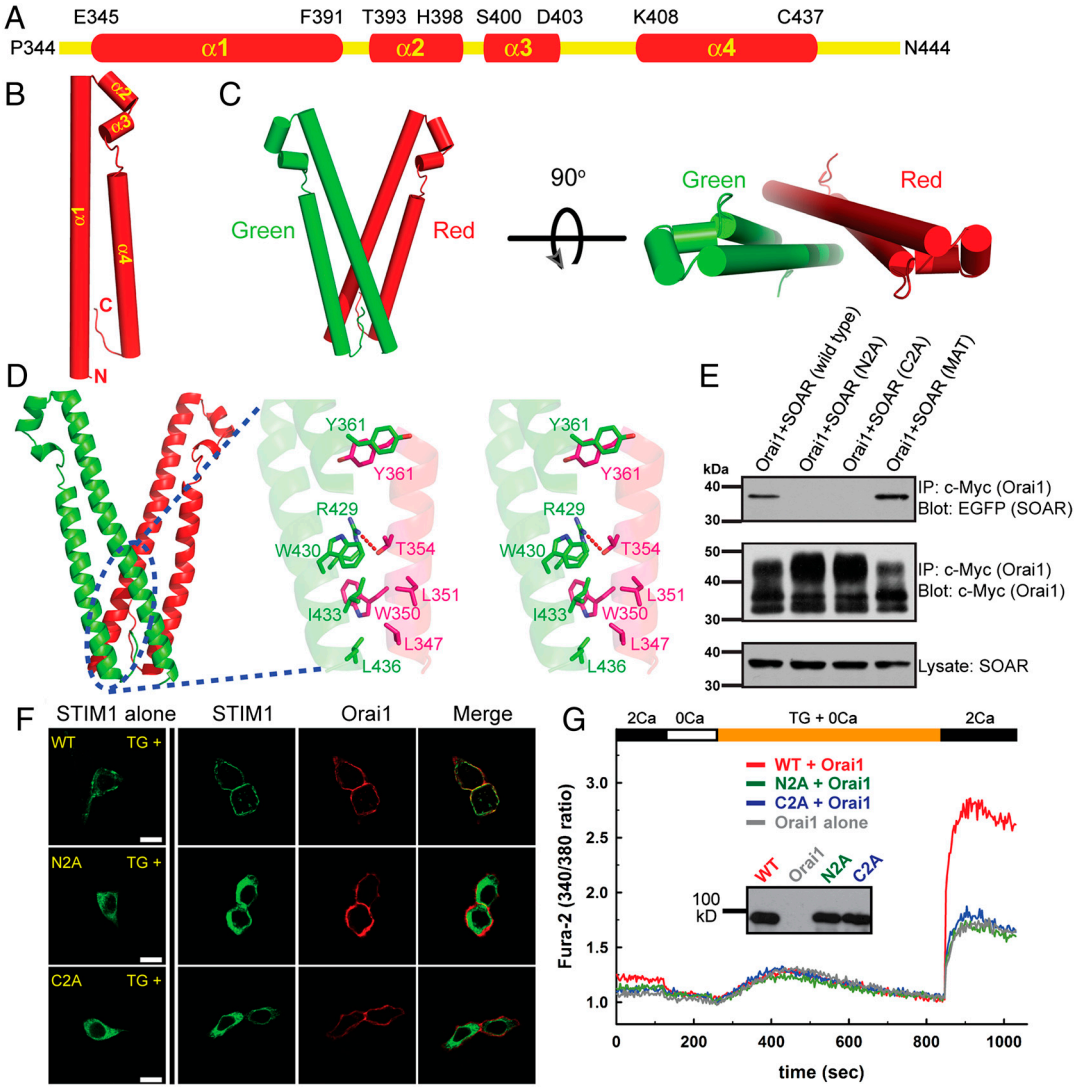

Fig. 1. SOAR dimer. (*A*) Schematic drawing of hSOAR. (*B*, *C*) Cartoon representation of the overall structure of the hSOAR monomer and the red-green hSOAR dimer. (*D*) Stereoview of the detailed interactions between the two monomers. The oxygen and nitrogen atoms are colored red and blue, respectively. Hydrogen bonds are shown by magenta dotted lines. (*E*) Western blots of coimmunoprecipitated wild-type and mutant hSOAR with the hOrai1 channel. (*F*) Localization of wild-type and mutant hSTIM1 transfected alone (first image in each row) and cotransfected with hOrai1. All hSTIM1 constructs were C-terminally tagged with EGFP and all hOrai1 constructs were N-terminally tagged with mCherry. Scale bars are 10 μm. (*G*) Fura-2 Ca^{2+} measurements of HeLa cells expressing hOrai1 alone or hOrai1 with wild-type or mutant hSTIM1. *Inset*, immunoblotting with anti-STIM1 antibody.

solution, whereas the hSOAR-MAT mutant only forms a dimer in solution. These results differ from a previous report that the CAD fragment of hSTIM1 exists primarily as a tetramer in solution (23). Structural analysis shows that four molecules of hSOAR in one asymmetric unit can be assembled into three types of dimers (red-blue, red-green, and red-cyan; Fig. S4). The buried surface area calculated by AREAIMOL (27) is 910.2 $Å^2$ for the red-blue dimer, 1775.9 $Å^2$ for the red-green dimer, and 825.9 $Å^2$ for the red-cyan dimer. Thus, the red-green dimer is the most stable packing unit among the three dimers and may represent the physiological dimer (Fig. 1*C*). Each of the blue and cyan molecules can also form a red-green dimer by a twofold noncrystallographic axis.

The red-green dimer has a V-shape, and the two monomers are packed by a 2-fold noncrystallographic axis (Fig. 1*D*, *Left*). At the dimer interface, the N- and C-termini from one monomer form a coiled-coil interaction with the C- and N-termini, respectively, from the other monomer (Fig. 1*D*, *Right*). First, residues Leu347, Trp350, and Leu351 from the red monomer form multiple hydrophobic interactions with residues Leu436, Ile433, and Trp430 from the green monomer. Second, residue Thr354 from the red monomer forms a hydrogen bond with residue Arg429 from the green monomer. Third, residue Tyr361 from the red monomer forms a stacking interaction with the same residue from the green monomer. All of these interactions occur vice versa. Moreover, all residues involved in interactions at the interface, except Tyr361 and Leu436, are identical in various species (Fig. S2), suggesting the evolutionary stability of this dimer.

To verify the physiological relevance of the red-green dimer, we made two mutants (L347A-W350A-L351A, referred to as N2A, and W430A-I433A-L436A, referred to as C2A) by mutating residues at the dimer interface to interfere with dimer formation. When coexpressed with hOrai1, wild-type hSOAR and its mutant hSOAR-MAT coimmunoprecipitate with hOrai1 (Fig. 1*E*) and colocalize with hOrai1 at the PM (Fig. S5). By contrast, the mutants (hSOAR-N2A and hSOAR-C2A) localize diffusely throughout the cytoplasm. When they are coexpressed with hOrai1, they neither coimmunoprecipitate (Fig. 1*E*) nor colocalize with hOrai1 at the plasma membrane (Fig. S5). These data indicate that correct assembly of the hSOAR dimer is crucial for binding with hOrai1. A recent study has demonstrated that N-and C-terminal truncated constructs of hSOAR do not bind hOrai1

(22). Furthermore, mutation of residues Leu347 and Gln348 in the N-terminal region of hSOAR also disrupts binding of hSOAR to hOrai1 (22). Our data are consistent with these findings.

We then created the same mutations on full-length hSTIM1 (hSTIM1-N2A and hSTIM1-C2A) and tested them for colocalization with hOrai1. Similar to the hSOAR results, wild-type hSTIM1 colocalizes with hOrai1 after TG treatment while hSTIM1-N2A and hSTIM1-C2A do not (Fig. 1*F*). To determine whether these two mutants affect SOCE in cells, we measured intracellular [Ca^{2+}] in HeLa cells expressing wild-type or mutant hSTIM1 and hOrai1. Wild-type hSTIM1 exhibits normal SOCE whereas both hSTIM1-N2A and hSTIM1-C2A mutants abolish SOCE (Fig. 1*G*). These results suggest that the hSOAR dimer observed in our structure most likely represents the correct assembly of full-length hSTIM1.

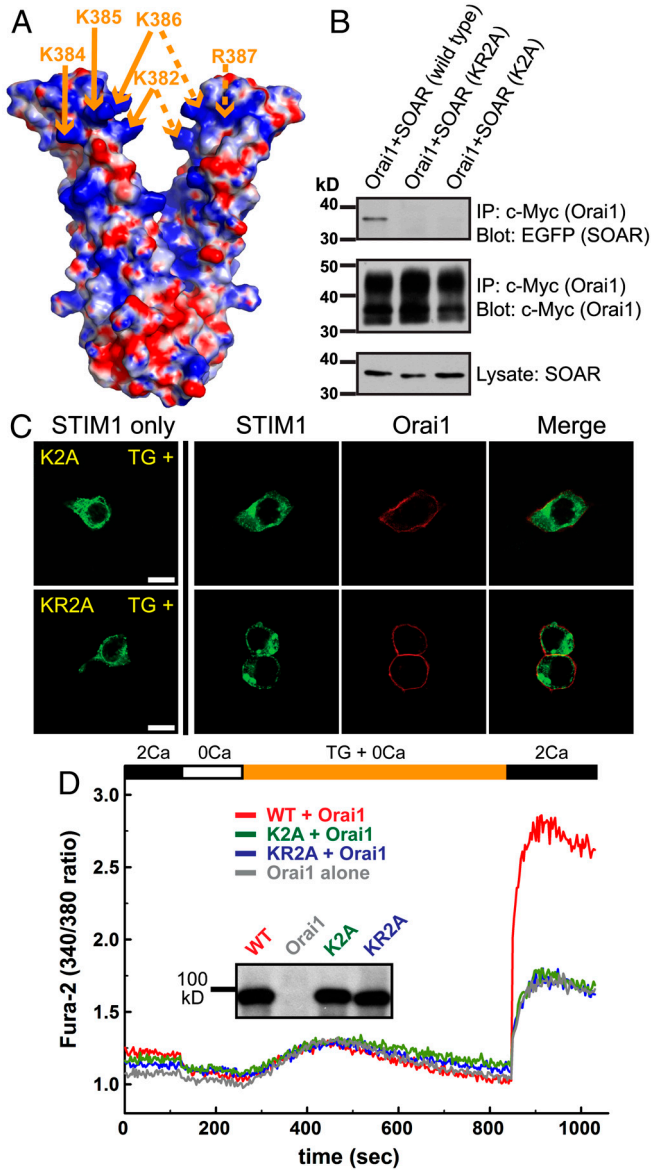

Fig. 2. Cluster of positive residues in hSOAR. (*A*) Electrostatic surface representation of the hSOAR dimer. The surface is colored as follows: negative, red; positive, blue; and neutral, white. The two monomers in the dimer are related by twofold noncrystallographic symmetry. For example, the Arg387 residue is located on the back of the left monomer and thus labeled on the surface of the right monomer. Two lysine residues (Lys384 and Lys385) are only displayed on the surface of the left monomer. (*B*) Western blots of hSOAR coimmunoprecipitated with the hOrai1 channel. (*C*) Localization of wild-type and mutant hSTIM1 tagged with EGFP transfected alone (first image in each row) and cotransfected with hOrai1 tagged with mCherry. Scale bars are 10 μm. (*D*) Fura-2 Ca^{2+} measurements of HeLa cells expressing hOrai1 alone or hOrai1 with wild-type or mutant hSTIM1. Inset, immunoblotting with anti-STIM1 antibody.

Cluster of Positively Charged Residues. To further address which part of hSOAR is necessary for binding of hSTIM1 to the hOrai1 channel, we calculated the electric potential distribution on the surface of the hSOAR dimer and found a positively charged patch at the C-terminus of helix α1 (Fig. 2*A*). This patch consists of five positively charged residues: Lys382, Lys384, Lys385, Lys386, and Arg387. A previous report showed that residues Lys384-386 of hSTIM1 are necessary for activating SOCE to gate Ca^{2+} influx by directly interacting with the negatively charged region of the C-terminal helix of hOrai1 (25, 28). Therefore, we hypothesized that these positive residues are crucial for binding of hSOAR to hOrai1. To verify this hypothesis, we made two hSOAR mutants to test their colocalization with hOrai1: one mutant replaced three lysine residues (Lys384-386) with alanines (referred to as K2A), and five positive residues (Lys382, Lys384-Arg387) were replaced with alanines (referred to as KR2A) in the other mutant. We then monitored the distribution of wild-type or mutant EGFP-hSOAR and mCherry-hOrai1 in HEK293T cells (Fig. S5). When coexpressed with hOrai1, these two mutants do not coimmunoprecipitate (Fig. 2*B*) or colocalize with hOrai1 at the plasma membrane (Fig. S5), indicating that the removal of this cluster of positive residues disrupts the interaction of hSOAR with hOrai1. As for the full-length hSTIM1, the wild-type protein colocalizes with hOrai1 and maintains normal SOCE, whereas the mutants hSTIM1-K2A and hSTIM1-KR2A do not (Fig. 2 *C* and *D*). Our data indicate that the cluster of positively charged residues located at the tip of the hSOAR dimer is necessary for binding of full-length hSTIM1 to the hOrai1 channel.

Overall Structure of ceSTIM1-CCR. As previously shown, the segment comprising residues 238–343 is the main inhibitory region that maintains hSOAR in an inactive state (25). To elucidate the mechanism of inhibition, we screened several constructs covering this inhibitory region plus different lengths of hSOAR (residues 238–444) from various sources. One of the constructs from *C. elegans* (Fig. 3*A*) produced a crystal that diffracted to 2.55 Å. The structure of ceSTIM1-CCR was solved by SAD methodology. The overall structure consists of three helices (αA-αC) (Fig. 3*B*). Two long helices (αB and αC) form a unit that is very similar to the hSOAR structure (Fig. S6*A*). There are two monomers in the asymmetric unit of ceSTIM1-CCR, and they pack into a dimer that is similar to the hSOAR dimer described above (Fig. 3*C* and Fig. S6). The ceSTIM1-CCR exists as a dimer in solution, as shown by an analytical ultracentrifugation (Fig. S7*A*). Unexpectedly, some of the N-terminal residues of ceSTIM1-CCR could not be modeled in the structure presumably due to a flexible conformation, as the dissolved crystal did not show any signs of degradation (Fig. S7*B*). Residues 257–279 of ceSTIM1-CCR, adjacent to SOAR from *C. elegans* (ceSOAR), form the αA helix (designated as the inhibitory helix) in the final structure (Fig. 3*B*). This inhibitory helix interacts with ceSOAR (Fig. 3*D*) in three ways. First, residues Glu264 and Asn265 of the inhibitory helix form several hydrogen bonds with residues Arg295 and Gln291 of the αB helix. Second, the side chains of residues Gln269, Glu272, and Arg276 from the inhibitory helix form hydrogen bonds with the main chain carbonyl groups of residues Leu288 and Ala286 from the αB helix and residues Gly383 and Cys382 from the αC helix. Third, residue Val268 from the inhibitory helix has a hydrophobic interaction with residue Pro385 from the αC helix. These interactions suggest that the inhibitory helix can tightly bind ceSOAR.

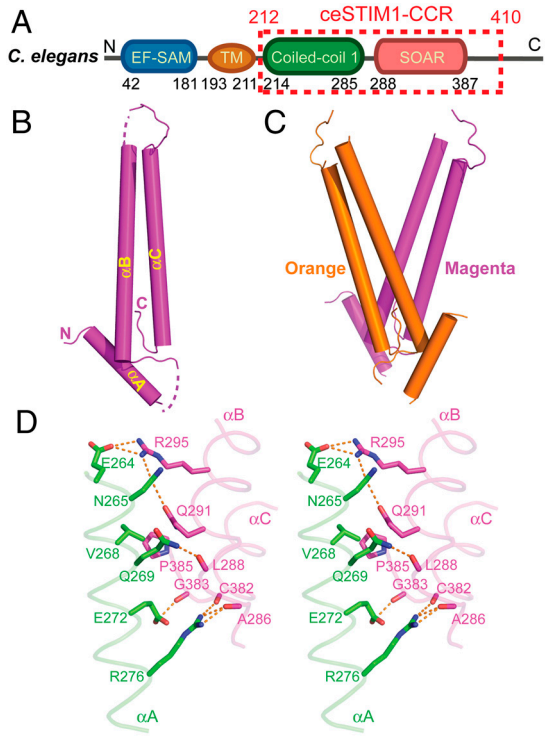

Fig. 3. Structure of ceSTIM1-CCR. (*A*) Schematic drawing of STIM1 from *C. elegans*. The ceSTIM1-CCR construct is shown in red. Overall structure of the ceSTIM1-CCR monomer (*B*) and dimer (*C*). Helix αA is named the inhibitory helix in this paper. (*D*) Stereoview of the detailed interactions between αA (green) and ceSOAR (helices αB and αC, magenta). The oxygen and nitrogen atoms are colored red and blue, respectively. Hydrogen bonds are shown by orange dotted lines.

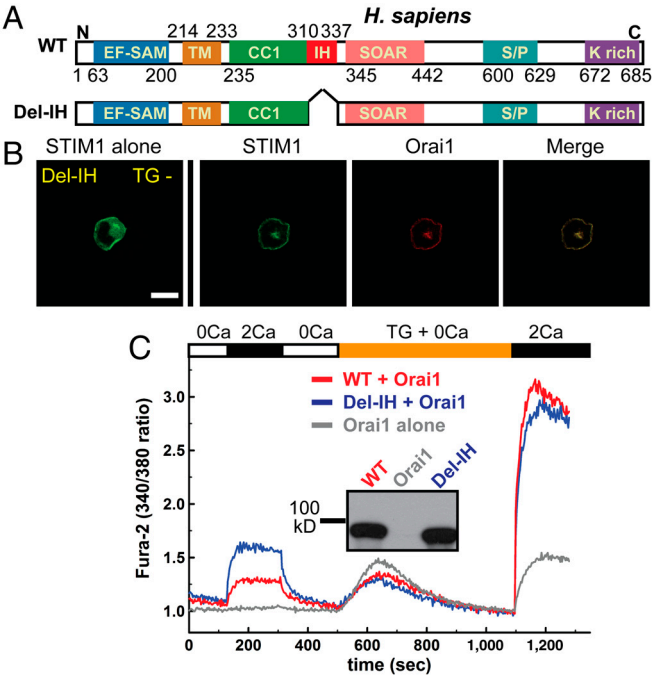

Fig. 4. The inhibitory helix maintains hSTIM1 in an inactive state. (*A*) Schematic drawing of wild-type and mutant STIM1 from *H. sapiens*. (*B*) Localization of hSTIM1 mutants transfected alone (first image in each row) and cotransfected with hOrai1 without TG treatment. Scale bars are 10 μm. (*C*) Fura-2 Ca^{2+} measurements of HeLa cells expressing hOrai1 alone or hOrai1 with wild-type or mutant hSTIM1. *Inset*, immunoblotting with anti-STIM1 antibody.

hSTIM1-CCR is in a Closed Conformation State. Functional studies have shown that *C. elegans* STIM1 (ceSTIM1) has a similar biological function to its human counterpart in terms of colocalization with the *C. elegans* Orai1 (ceOrai1) channel and a normal SOCE (Fig. S8), consistent with previous reports (29). In addition, there is high sequence homology between human and worm STIM1 (Fig. S9). Thus, we hypothesized that residues 310–337 of human STIM1-CCR, corresponding to the inhibitory helix of *C. elegans*, may act as an inhibitory unit to keep hSTIM1 in an inactive resting state.

To test this hypothesis, we constructed a hSTIM1 mutant lacking the inhibitory helix (referred to as Del-IH, Fig. 4*A*), which should keep hSTIM1 constitutively active independently of calcium store depletion. Indeed, Del-IH colocalizes with hOrai1 without TG treatment (Fig. 4*B*) and is constitutively active according to intracellular calcium measurements (Fig. 4*C*). Korzeniowski and coworkers have reported that a hSTIM1 mutant with four Glu to Ala mutations (E318A-E319A-E320A-E322A) is a constitutively active mutant (25). We found that the Glu264 residue in ceSTIM1, which corresponds to Glu322 in hSTIM1, is located in the inhibitory helix and is involved in the interaction with ceSOAR (Fig. 3*D*, and Fig. S9). Our experiments suggest that the inhibitory helix keeps hSTIM1 inactive.

Discussion

The present study describes the atomic structure of the hSOAR domain of hSTIM1, revealing that the hSOAR dimer is most likely a necessary unit for biological functions. Mutations that interfere with the formation of the hSOAR dimer or remove the positively charged cluster in the hSOAR dimer abolish the ability of hSOAR to activate the Orai1 channel. Similar mutations in full-length hSTIM1 abolish normal SOCE after calcium store depletion. Consistent with our results, the hSTIM1 construct (amino acids 233–420) that did not encompass the entire hSOAR domain in hSTIM1-C is clearly a monomer in solution and neither localizes to the PM nor homomerizes when coexpressed with hOrai1 (30). Previous researchers have reported that the functional hOrai1 channel exists as a tetramer (31). Ji and coworkers reported that the CRAC channel complex consists of four hOrai1 molecules and two hSTIM1 molecules (32). Recent research has shown that maximal hOrai1 channel activity requires binding of one hSTIM1 dimer to each of the four sites of the functional hOrai1 channel (33, 34). Therefore, we think the hSOAR dimer observed in our structure most likely represents the correct assembly of the hSTIM1 dimer. Upon activating the hOrai1 channel, hSTIM1 further packs into a higher order oligomer using a dimer as a basic unit (11).

In a resting state, hSTIM1 may exist mostly as dimers (31). A purified wild-type hSTIM1 construct (residues 234–491) exists as a dimer in solution (26). Consistent with these findings, our crystallographic and solution data suggest that hSTIM1 is mainly a dimer in its inactive state. Our structural and functional data also show a possible inhibitory helix that interacts tightly with the hSOAR dimer and thus keeps hSTIM1 inactive. This inhibitory helix may undergo conformational changes to release the hSOAR dimer upon hSTIM1 activation and the structure of SOAR may change to be favorable for interacting with Orai1. Our findings differ from the previous electrostatic model in which the acidic segment in the first coiled-coil domain of hSTIM1 mediates an intramolecular interaction with the polybasic segment in the hSOAR domain to keep hSTIM1 inactive (25, 35). Our crystal structures suggest that the polybasic and acidic segments are less likely to interact with each other because the polybasic segment is located on the tip of the V-shaped hSOAR dimer while the acidic segment is partially involved in the interaction with the bottom part of the V-shaped hSOAR dimer.

Our results, together with those of previous studies, allowed us to develop a working model for the activation of the C-terminus

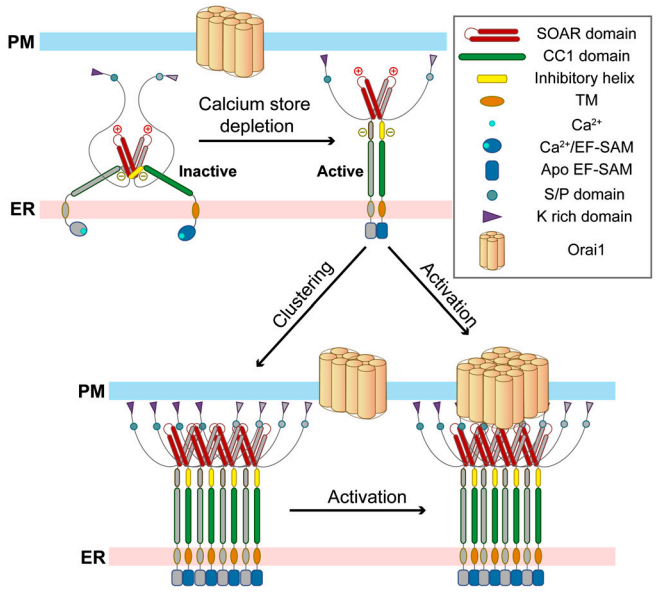

Fig. 5. Model of STIM1 activation. In the resting state, the STIM1 molecule mainly exists as a dimer. The SOAR dimer is likely occluded by the inhibitory helices and the region consisting of amino acids 486–685. Calcium depletion from the ER store induces dimerization or oligomerization of STIM1-N, causing conformational changes of inhibitory helices and thus release of dimeric SOAR. The STIM1 dimer in the active state may directly couple to and activate the Orai1 channel on the PM. Alternatively, STIM1 molecules may oligomerize due to aggregation of STIM1-N and then activate the Orai1 channel.

of hSTIM1 (Fig. 5). In a resting state, hSTIM1 may exist mostly as dimers. The hSOAR dimer is possibly occluded by the inhibitory helix. One region of the hSTIM1 molecule (residues 486–685) may inhibit hSOAR dimer formation by steric hindrance (22, 25, 36). Calcium-bound hSTIM1-N within the ER remains monomeric (16). At this stage, the entire hSTIM1-C region forms a compact conformational state, called the "inactive" state. After calcium store depletion, hSTIM1-N releases bound calcium and dimerizes or oligomerizes (16). This oligomerization causes conformational changes, leading residues 238–343 to form an elongated coiled coil and thus release hSOAR from the inhibitory helix, as supported by Förster resonance energy transfer (FRET) studies of the OASF segment (YFP-233-474-CFP). Indeed, OASF undergoes a conformational change from a compact to an extended conformation when coexpressed with hOrai1 (26). The hSOAR dimer can then change the conformation. The extended conformation of hSTIM1-C may induce binding of the poly-Lys region (672–685) at the carboxyl end of hSTIM1-C to membrane phospholipids (11), further exposing the hSOAR dimer. The K/R-rich region (365–387) of hSTIM1 may facilitate movement of the hSOAR dimer towards the PM to look for the hOrai1 channel. Covington et al. reported that this positively charged region possibly interacts with the PM because STIM1-CAD (1–448) localizes to ER-PM junctions after depletion when expressed alone (11). At this stage, the entire hSTIM1-C is in an extended conformational state, designated as the "active" state. The hSTIM1-C uses the exposed hSOAR dimer to bind to the hOrai1 channel on the PM and to induce cooperative binding of more hSTIM1 dimers to the hOrai1 channel, which causes opening of the hOrai1 channel (33, 34). However, hSTIM1-C in the "active" state may oligomerize with other hSTIM1 molecules due to aggregation of hSTIM1-N.

The activation of hSTIM1-C is a complicated process and may be regulated by other effectors. For example, CRACR2A closely interacts with hSTIM1-C and hOrai1 and may be an important regulator (37). In addition to its role as an ER calcium sensor, hSTIM1 has recently been recognized as a sensor of oxidative stress (13) and temperature variation (14). The trigger of hSTIM1-N oligomerization may be different, but hSTIM1-C seems to share a conserved molecular mechanism to activate the hOrai1 channel (35). Our model may represent a basic process for the activation of hSTIM1-C. Other effectors may modulate this process to fulfill the complicated task of store-operated calcium entry.

Materials and Methods

Protein purification and structure determination. Human SOAR (residues 345–444) and *C. elegans* STIM1 (residues 212–410) were expressed in *Escherichia coli* and purified by chromatographic methods. Structures of hSOAR and ceSTIM1-CCR were determined by SAD methodology. The experimental methods are described in full in the *Supporting Information*. Detailed data collection and refinement statistics are summarized in Table S1. Representative electron density maps are shown in Fig. S10.

Cell Culture and Transfection. HEK293T and HeLa cells (ATCC) were cultured in Dulbecco's modified Eagle's medium (DMEM, Sigma-Aldrich) supplemented with 10% v/v fetal bovine serum (FBS, HyClone Thermo Fisher Scientific). Cells were maintained in a 95% air and 5% CO_2 environment at 37 °C. Gene fragments corresponding to the full-length hSTIM1 and ceSTIM1 were cloned into a pEGFP-N1 vector (Clontech). The mutants (K2A, KR2A, N2A, C2A, and Del-IH) were made using a standard PCR-based mutagenesis method and confirmed by DNA sequencing. Gene fragments of hSOAR were cloned into pEGFP-N1 and pmCherry-C1 vectors (Clontech). hOrai1 was cloned into pmCherry-C1, pCMV-myc, and pECFP-N1 vectors (Clontech). ceOrai1 was cloned into the pmCherry-C1 vector. The YFP-HA-$Ca_V1.2$ construct was a gift from Ricardo Dolmetsch (Stanford University).

Confocal Imaging. Cells were cultured on glass coverslips in a 24-well plate format and transfected at 70% confluency with 0.5 μg of DNA per well using Lipofectamine 2000 (Invitrogen) according to the manufacturer's instructions. Cells were imaged in 2 mM Ca^{2+} Ringer's solution containing 145 mM NaCl, 1 mM $MgCl_2$, 4.5 mM KCl, 10 mM D-glucose, 20 mM Hepes pH 7.4 and 2 mM $CaCl_2$. For store depletion, cells were perfused with Ca^{2+}-free Ringer's solution prepared with 1 μM thapsigargin (TG; Sigma-Aldrich), 145 mM NaCl, 1 mM $MgCl_2$, 1 mM EGTA, 4.5 mM KCl, 10 mM D-glucose and 20 mM Hepes pH 7.4.

The cells were fixed with 4% paraformaldehyde and mounted onto microscope slides. EGFP, mCherry, and YFP were excited at 488, 543, and 514 nm, respectively, on a Leica TCS SP5 inverted confocal microscope. Fluorescence emission was detected at 510–570 nm (EGFP), 590–650 nm (mCherry), and 525–575 (YFP).

Coimmunoprecipitation and Western Blotting. Transfected HEK293T cells were collected in PBS. Cells were lysed in buffer containing 20 mM Tris-HCl, pH 7.5, 2 mM EDTA, 100 mM NaCl, 10% glycerol, 0.5% Triton X-100, and protease inhibitor cocktail (Roche) and centrifuged at 16,000 × *g* for 1 h. Anti-c-Myc antibody (1 μg) was added to the cell extract (300 μL) and incubated for 1 h at 4 °C. Fifty microliters of a 1:1 slurry of protein A/G Agarose (Pierce) was added to the antibody-extract mixture, which was incubated for an additional hour at 4 °C. The beads were washed three times for 10 min with binding buffer, followed by addition of 40 μL of SDS-loading buffer. Then, 10 μL of the solution was loaded onto a 12% SDS-PAGE gel and transferred onto a PVDF membrane for western blot analysis. Immunoblot analysis was carried out with mouse anti-GFP as a primary antibody and HRP-conjugated goat anti-mouse IgG as a secondary antibody. The protein/antibody complexes were detected by enhanced chemiluminescence.

Intracellular Calcium Measurement. HeLa cells were plated onto a 24-well plate (Costar) and transfected at 90% confluency with 0.7 μg DNA per well using Lipofectamine 2000. Transfected cells were loaded with 1 μM Fura-2 AM (Sigma-Aldrich) in DMEM with 10% FBS for 30 min at 37 °C. After loading, the cells were rinsed in 2 mM Ca^{2+} Ringer's solution containing 145 mM NaCl, 1 mM $MgCl_2$, 4.5 mM KCl, 10 mM glucose, 20 mM Hepes pH 7.4 and 2 mM $CaCl_2$ for 20 min. Excitation at 340 nm and 380 nm, emissioned at 508 nm and monitored using a Synergy4 spectrometer (BioTek). Data representing relative intracellular Ca^{2+} concentrations are reported as 340/380 ratios.

ACKNOWLEDGMENTS. We are grateful to Dr. Xiangdong Tang in School of Medicine at Nankai University for providing the cDNA of human Orai1 and human STIM1, to Mr. Zheng Wang for technique assistance in analytical ultracentrifuge experiment, to the staff at the beamline BL17U1 of the

Shanghai Synchrotron Radiation Facility for excellent technical assistance during data collection. This work was funded by the 973 Program (Grants 2009CB825504 and 2012CB917201), National Nature Science Foundation of China (Grant 31170684), Tianjin Basic Research program (Grants 08QTPTJC28200 and 08SYSYTC00200) and the Fundamental Research Funds for the Central Universities (Grant 65020241).

1. Clapham DE (2007) Calcium signaling. *Cell* 131:1047–1058.
2. Hogan PG, Lewis RS, Rao A (2010) Molecular basis of calcium signaling in lymphocytes: STIM and ORAI. *Annu Rev Immunol* 28:491–533.
3. Feske S (2010) CRAC channelopathies. *Pflugers Arch* 460:417–435.
4. Liou J, et al. (2005) STIM is a Ca^{2+} sensor essential for Ca^{2+}-store-depletion-triggered Ca^{2+} influx. *Curr Biol* 15:1235–1241.
5. Roos J, et al. (2005) STIM1, an essential and conserved component of store-operated Ca^{2+} channel function. *J Cell Biol* 169:435–445.
6. Feske S, et al. (2006) A mutation in Orai1 causes immune deficiency by abrogating CRAC channel function. *Nature* 441:179–185.
7. Vig M, et al. (2006) CRACM1 multimers form the ion-selective pore of the CRAC channel. *Curr Biol* 16:2073–2079.
8. Prakriya M, et al. (2006) Orai1 is an essential pore subunit of the CRAC channel. *Nature* 443:230–233.
9. Lewis RS (2007) The molecular choreography of a store-operated calcium channel. *Nature* 446:284–287.
10. Vig M, Kinet JP (2009) Calcium signaling in immune cells. *Nat Immunol* 10:21–27.
11. Covington ED, Wu MM, Lewis RS (2010) Essential role for the CRAC activation domain in store-dependent oligomerization of STIM1. *Mol Biol Cell* 21:1897–1907.
12. Feske S (2007) Calcium signalling in lymphocyte activation and disease. *Nat Rev Immunol* 7:690–702.
13. Hawkins BJ, et al. (2010) S-glutathionylation activates STIM1 and alters mitochondrial homeostasis. *J Cell Biol* 190:391–405.
14. Xiao B, Coste B, Mathur J, Patapoutian A (2011) Temperature-dependent STIM1 activation induces $Ca^{(2)+}$ influx and modulates gene expression. *Nat Chem Biol* 7:351–358.
15. Mancarella S, Wang Y, Gill DL (2011) Signal transduction: STIM1 senses both $Ca^{(2)+}$ and heat. *Nat Chem Biol* 7:344–345.
16. Stathopulos PB, et al. (2008) Structural and mechanistic insights into STIM1-mediated initiation of store-operated calcium entry. *Cell* 135:110–122.
17. Fahrner M, et al. (2009) Mechanistic view on domains mediating STIM1-Orai coupling. *Immunol Rev* 231:99–112.
18. Stathopulos PB, et al. (2006) Stored Ca^{2+} depletion-induced oligomerization of stromal interaction molecule 1 (STIM1) via the EF-SAM region: An initiation mechanism for capacitive Ca^{2+} entry. *J Biol Chem* 281:35855–35862.
19. Baba Y, et al. (2006) Coupling of STIM1 to store-operated Ca^{2+} entry through its constitutive and inducible movement in the endoplasmic reticulum. *Proc Natl Acad Sci USA* 103:16704–16709.
20. Liou J, Fivaz M, Inoue T, Meyer T (2007) Live-cell imaging reveals sequential oligomerization and local plasma membrane targeting of stromal interaction molecule 1 after Ca^{2+} store depletion. *Proc Natl Acad Sci USA* 104:9301–9306.
21. Zhou Y, et al. (2010) STIM1 gates the store-operated calcium channel ORAI1 in vitro. *Nat Struct Mol Biol* 17:112–116.
22. Yuan JP, et al. (2009) SOAR and the polybasic STIM1 domains gate and regulate Orai channels. *Nat Cell Biol* 11:337–343.
23. Park CY, et al. (2009) STIM1 clusters and activates CRAC channels via direct binding of a cytosolic domain to Orai1. *Cell* 136:876–890.
24. Kawasaki T, Lange I, Feske S (2009) A minimal regulatory domain in the C terminus of STIM1 binds to and activates ORAI1 CRAC channels. *Biochem Biophys Res Commun* 385:49–54.
25. Korzeniowski MK, Manjarres IM, Varnai P, Balla T (2010) Activation of STIM1-Orai1 involves an intramolecular switching mechanism. *Sci Signal* 3:ra82.
26. Muik M, et al. (2011) STIM1 couples to ORAI1 via an intramolecular transition into an extended conformation. *EMBO J* 30:1678–1689.
27. Lee B, Richards FM (1971) The interpretation of protein structures: Estimation of static accessibility. *J Mol Biol* 55:379–400.
28. Calloway N, Holowka D, Baird B (2010) A basic sequence in STIM1 promotes Ca^{2+} influx by interacting with the C-terminal acidic coiled coil of Orai1. *Biochemistry* 49:1067–1071.
29. Gao S, et al. (2009) Mechanism of different spatial distributions of Caenorhabditis elegans and human STIM1 at resting state. *Cell Calcium* 45:77–88.
30. Muik M, et al. (2009) A cytosolic homomerization and a modulatory domain within STIM1 C terminus determine coupling to ORAI1 channels. *J Biol Chem* 284:8421–8426.
31. Penna A, et al. (2008) The CRAC channel consists of a tetramer formed by Stim-induced dimerization of Orai dimers. *Nature* 456:116–120.
32. Ji W, et al. (2008) Functional stoichiometry of the unitary calcium-release-activated calcium channel. *Proc Natl Acad Sci USA* 105:13668–13673.
33. Li Z, et al. (2011) Graded activation of CRAC channel by binding of different numbers of STIM1 to Orai1 subunits. *Cell Res* 21:305–315.
34. Hoover PJ, Lewis RS (2011) Stoichiometric requirements for trapping and gating of Ca^{2+} release-activated Ca^{2+} (CRAC) channels by stromal interaction molecule 1 (STIM1). *Proc Natl Acad Sci USA* 108:13299–13304.
35. Soboloff J, Madesh M, Gill DL (2011) Sensing cellular stress through STIM proteins. *Nat Chem Biol* 7:488–492.
36. Yu F, Sun L, Courjaret R, Machaca K (2011) Role of the STIM1 C-terminal domain in STIM1 clustering. *J Biol Chem* 286:8375–8384.
37. Srikanth S, et al. (2010) A novel EF-hand protein, CRACR2A, is a cytosolic Ca^{2+} sensor that stabilizes CRAC channels in T cells. *Nat Cell Biol* 12:436–446.